LIMNOLOGY
and
OCEANOGRAPHY

ASLO

Limnol. Oceanogr. 61, 2016, 1188–1200

doi: 10.1002/lno.10266

Dynamics of extracellular superoxide production by *Trichodesmium* colonies from the Sargasso Sea

C. M. Hansel,*[1] C. Buchwald,[1] J. M. Diaz,[a1] J. E. Ossolinski,[1] S. T. Dyhrman,[2] B. A. S. Van Mooy,[1] Despo Polyviou[3]

[1]Department of Marine Chemistry and Geochemistry, Woods Hole Oceanographic Institution, Woods Hole, Massachusetts
[2]Department of Earth and Environmental Science and Lamont-Doherty Earth Observatory, Columbia University, New York, New York
[3]Ocean and Earth Sciences, National Oceanography Centre Southampton, University of Southampton, Waterfront Campus, Southampton, United Kingdom

Abstract

Reactive oxygen species (ROS) are key players in the health and biogeochemistry of the ocean and its inhabitants. The vital contribution of microorganisms to marine ROS levels, particularly superoxide, has only recently come to light, and thus the specific biological sources and pathways involved in ROS production are largely unknown. To better understand the biogenic controls on ROS levels in tropical oligotrophic systems, we determined rates of superoxide production under various conditions by natural populations of the nitrogen-fixing diazotroph *Trichodesmium* obtained from various surface waters in the Sargasso Sea. *Trichodesmium* colonies collected from eight different stations all produced extracellular superoxide at high rates in both the dark and light. Colony density and light had a variable impact on extracellular superoxide production depending on the morphology of the *Trichodesmium* colonies. Raft morphotypes showed a rapid increase in superoxide production in response to even low levels of light, which was not observed for puff colonies. In contrast, superoxide production rates per colony decreased with increasing colony density for puff morphotypes but not for rafts. These findings point to *Trichodesmium* as a likely key source of ROS to the surface oligotrophic ocean. The physiological and/or ecological factors underpinning morphology-dependent controls on superoxide production need to be unveiled to better understand and predict superoxide production by *Trichodesmium* and ROS dynamics within marine systems.

Reactive oxygen species (ROS) are important players in the biogeochemistry of the ocean, where they serve a critical role in the cycling of carbon and metals. For instance, the ROS, superoxide ($O_2^{\bullet-}$) and hydrogen peroxide (H_2O_2), are capable of oxidizing and/or reducing a number of metals, including copper (Cu), iodine (I), and manganese (Mn) (Archibald and Fridovich 1982; Voelker et al. 2000; Hansard et al. 2011; Learman et al. 2013; Wuttig et al. 2013; Li et al. 2014). Importantly, superoxide also has the ability to reduce Fe(III) to Fe(II) (Voelker and Sedlak 1995; Rose 2012). As Fe is an essential nutrient that limits photosynthesis in vast regions of the ocean, superoxide-mediated reduction and subsequent release of Fe from strong Fe(III)-ligands has been suggested as an important process controlling biological activity in the surface ocean (Rose et al. 2005). Unlike superoxide, hydrogen peroxide is an important oxidant of Fe(II) (Moffett and Zika 1987; Millero and Sotolongo 1989), which also leads to the formation of the highly reactive hydroxyl radical, a ROS that rapidly degrades carbon, including recalcitrant forms such as lignin.

All aerobic organisms form ROS intracellularly as a byproduct of respiration or photosynthesis. Oxidative stress involves the accumulation of these ROS to toxic levels within the cell, where the ROS alter the redox state of critical enzymes or destroy essential biomolecules, such as membranes and proteins. Since ROS other than H_2O_2 have limited ability to passively diffuse or be actively transported across biological membranes (Korshunov and Imlay 2002), organisms must deal with these toxic molecules internally. Thus, to minimize cellular damage, and evade death, levels

*Correspondence: chansel@whoi.edu

[a]Present address: Skidaway Institute of Oceanography, Department of Marine Sciences, University of Georgia, Savannah, Georgia

Competing financial interests: The authors declare no competing financial interests.

Additional Supporting Information may be found in the online version of this article.

of intracellular ROS are highly regulated through the production of molecules and enzymes that specifically target and destroy oxygen radicals (Fridovich 1998). These antioxidants include enzymes such as superoxide dismutase (SOD), catalase, and peroxidase, and small molecules such as glutathione.

ROS, particularly superoxide, are also produced extracellularly by a broad range of microorganisms, including fungi, phytoplankton, and bacteria (Aguirre et al. 2005; Kustka et al. 2005; Marshall et al. 2005; Rose et al. 2008b; Learman et al. 2011; Hansel et al. 2012; Rose 2012; Diaz et al. 2013; Tang et al. 2013). Research in the past decade has introduced phytoplankton and, most recently, heterotrophic bacteria as significant sources of ROS, including superoxide. Despite what appears to be a widespread ability of organisms to produce extracellular superoxide, the full repertoire of reasons for this process remains unclear. In fungi, this extracellular production is known to mediate a number of essential physiological processes, including cell development and signaling. It is widely appreciated, for instance, that cell differentiation in fungi is controlled by superoxide production via transmembrane NADPH oxidases (Bedard et al. 2007; Tsukagoshi et al. 2010). Similar enzymes have been implicated in superoxide production by the diatoms *Thalassiosira weissflogii* and *Thalassiosira pseudonana* (Kustka et al. 2005), the coral algal symbiont *Symbiodinium* sp. (Saragosti et al. 2010), and the toxic raphidophyte *Chattonella* (Kim et al. 2000). The reasons for bacterial and phytoplankton extracellular superoxide production remain unclear, but may include cellular warfare as proposed for *Chattonella marina* (Oda et al. 1992) or iron acquisition as observed in the marine cyanobacterium *Lyngbya* (Rose et al. 2005; Rose 2012).

Filamentous dinitrogen-fixing cyanobacteria in the genus *Trichodesmium* have demonstrated the ability to produce extracellular superoxide in a laboratory strain and in *Trichodesmium*-bearing coastal bloom waters (Godrant et al. 2009; Rose et al. 2010). *Trichodesmium* spp. occur throughout the oligotrophic tropical and subtropical ocean where it exists as both single trichomes and multi-trichome colonies (Capone et al. 1997). These colonies come in a variety of morphologies, including spherical puffs, fusiform tufts/rafts (twisted/flat filaments), and bowties (Hynes et al. 2012). Extracellular superoxide production has recently been implicated in enhanced iron uptake in *Trichodesmium*, and may therefore be an essential strategy utilized by this species to acquire iron in the ocean (Roe and Barbeau 2014). Conversely, oxidative stress and intracellular superoxide production has also been implicated in initiating programmed cell death (PCD) within *Trichodesmium* colonies (Berman-Frank et al. 2004, 2007). Despite the importance of superoxide to the growth and activity of *Trichodesmium*, the conditions promoting extracellular production are largely unknown and unexplored in oligotrophic environments. Further, *Trichodesmium* blooms oftentimes also contain high abundances of other plankton, including, for instance, the widespread diatom *Coscinodiscus* (Karthik et al. 2012), that may contribute to ROS cycling within the bloom community. Accordingly, the goals of this study were to measure rates of superoxide production by natural *Trichodesmium* populations and associated diatoms obtained from various surface waters in the Sargasso Sea and to evaluate how these activities were modulated.

Sample collection and methods

Sample collection

Natural *Trichodesmium* colonies were collected on a cruise (AE1409) within the tropical western North Atlantic Ocean on the R/V *Atlantic Explorer* from 09 May 2014 to 27 May 2014. Colonies were collected from the near surface (upper ~25 m) using a 130 μm plankton net at eight stations along a transect from Bermuda to Barbados (see Fig. 1). Individual colonies were gently picked using a transfer pipet, sorted into puffs vs. rafts, and sequentially washed three times in 0.2 μm filtered seawater. Colonies of visibly similar size were picked to attempt to minimize cell abundance variability in superoxide measurements. The puffs and rafts were either measured individually at different colony densities, or combined at various ratios to evaluate the influence of mixed morphology samples. All analyses were performed within 3 h of collection. At Stations 14 and 16, harvested plankton colonies contained a high proportion of the solitary diatom *Coscinodiscus*. Transfer of the plankton net community to a clear bucket allowed for easy separation of suspended *Trichodesmium* colonies and visible *Coscinodiscus* cells which sank to the bottom of the bucket. *Coscinodiscus* cells were harvested also using a transfer pipet and sequentially washed to remove (or minimize) other plankton communities.

Superoxide measurements

Trichodesmium colonies and *Coscinodiscus* cells were gently added by transfer pipet (*Trichodesmium*) or peristaltic pump (*Coscinodiscus*) to 5 μm filters within a Swinex holder and placed in-line of an FeLume Mini system (Waterville Analytical, Waterville, Maine) (see below for detail). Extracellular superoxide was measured by running 0.2 μm aged filtered seawater (AFSW) past the filter-supported colonies directly into the instrument where it was mixed with the superoxide-specific chemiluminescent probe methyl *Cypridina* luciferin analog (MCLA) as described in detail previously (Diaz et al. 2013) (see Supporting Information Fig. S1 for simplified schematic).

In detail, the FeLume system is composed of two separate fluid lines, one of which is dedicated to the analyte solution and the other to the MCLA reagent. Both solutions are independently flushed through the system at an identical flow rate using a peristaltic pump until they converge in a spiral flow cell immediately adjacent to a photomultiplier tube, which continuously acquires data that is displayed in real time using a PC interface. Similar systems have been used to

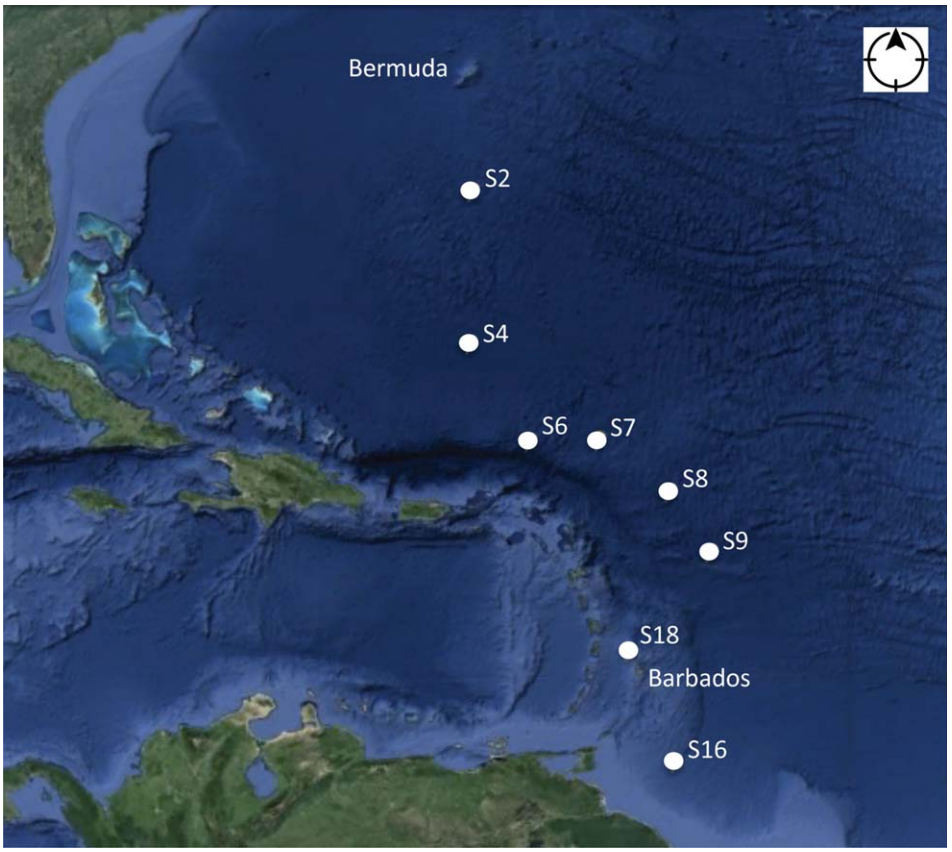

Fig. 1. Map of the tropical western North Atlantic Ocean showing the eight stations included in this research.

generate high sensitivity measurements of natural superoxide concentrations and decay rates (Rose et al. 2008a; Hansard et al. 2010), as well as extracellular superoxide production by bacteria (Diaz et al. 2013) and phytoplankton isolates (Kustka et al. 2005; Rose et al. 2008b). To eliminate potential photogenic sources of superoxide in our experiments, the entire FeLume system was shielded from ambient light using opaque tubing and a professional-grade dark bag designed for changing photography film.

For calibration, primary standard solutions of potassium dioxide (KO_2) were prepared in NaOH (pH = 12.5) amended with 90 μM diethylene-triaminepentaacetic acid (DTPA) to sequester trace contaminants that would otherwise significantly reduce the lifetime of superoxide. Superoxide concentrations in primary standards were quantified by measuring the difference in absorbance at 240 nm before and after the addition of superoxide dismutase (SOD; $\sim$2 U mL^{-1}) and then converting to molar units based on the molar absorptivity of superoxide corrected for the absorption of hydrogen peroxide formed during decay at the same wavelength (Bielski et al. 1985). To create secondary standards for analysis on the FeLume, these solutions were further diluted with AFSW amended with 50 μM DTPA, as described in more detail below. Before introducing superoxide standards to the FeLume, an in-line filter (0.22 μm; cellulose-acetate or polyethersulfone) was placed in the analyte line, where it remained throughout the duration of the experiment. (This was done to provide consistency with biological experiments, see below.) Next, the plain carrier solution was allowed to pass across the filter and react with the MCLA reagent (4.0 μM MCLA, 50 μM DTPA, 0.10 M MES, pH = 6.0) until a stable baseline (< 4% coefficient of variation) was achieved for $\sim$1 min. Then the secondary standards were pumped directly through the analyte line across the in-line syringe filter. The analyte and reagent were each pumped at a flow rate of 2.00 ± 0.05 mL min^{-1}, which was confirmed gravimetrically. Because superoxide is unstable, both primary and secondary standards were used immediately after preparation.

To prepare calibration curves, the chemiluminescence signal generated from the secondary standards was baseline-corrected for the chemiluminescence signal arising from the autooxidation of the MCLA reagent and extrapolated back to the time at which the primary standard was diluted ($t = 0$). Baseline correction was achieved by subtracting the average background signal generated from the AFSW carrier solution passing over the in-line filter, without KO_2, and reacting with the MCLA reagent for at least 1 min, as described

above. Baseline-corrected chemiluminescence data collected over several minutes of superoxide decay in standard solutions were log-linear and therefore modeled using pseudo-first order decay kinetics. The half-life of superoxide in most experiments was approximately 2.5 min or less. Standard signals were typically measured on the FeLume approximately 1 min after spectrophotometric quantification of standard stocks, a significant amount of time relative to the timescale of superoxide decay. Chemiluminescence data were therefore extrapolated backward in time to model time-zero chemiluminescence signals.

Daily calibration curves were generated from three paired observations of time-zero superoxide concentration (dependent variable) and extrapolated chemiluminescence (independent variable) using linear regression. Because chemiluminescence values were baseline-corrected, regression lines were forced through the origin. Calibrations yielded highly linear curves (e.g., $R^2 > 0.9$), with a typical sensitivity of 0.5 chemiluminescence units per pM superoxide (median).

As in calibration experiments, a clean filter (25 mm; 0.22 μm; cellulose-acetate or polyethersulfone) was placed downstream of the peristaltic pump and upstream of the flow cell in the analyte line, where it remained throughout the duration of the experiment. Stable baseline signals ($< 4\%$ coefficient of variation) were generated in biological experiments from AFSW passing over the in-line filter and reacting with MCLA for at least 1 min. The AFSW, which served as the carrier solution and baseline, was prepared at various stations along the transect. The seawater was amended with 50 μM DTPA to complex metals that would shorten the lifetime of ROS and filtered (0.2 μm) and aged in the dark for 2 d to allow for complete decay of endogenous ROS. The pump was temporarily stopped and *Trichodesmium* colonies were added to the in-line filter using a transfer pipet to the desired cell density. For *Coscinodiscus*, cells were gently pumped directly through the analyte line at a flow rate of 2 mL min^{-1}, and cells were deposited onto the in-line syringe filter as conducted previously for bacteria (Diaz et al. 2013). Microscopic examination of the cells post analysis did not indicate visible cellular damage. The presence of cells did not alter flow rates during the experiment, as flow rates after cell addition were within the analytical error of the rate determined beforehand. Extracellular superoxide produced by the organisms housed on the in-line filter and released into the AFSW carrier solution was detected downstream upon mixing with the MCLA reagent in the flow cell. Chemiluminescence signals yielded in biological experiments were considered stable on achieving a coefficient of variation (CV) equal to or less than that of the baseline for at least 1 min ($CV \leq \pm 4\%$). These signals were corrected for background chemiluminescence by subtracting the average baseline obtained immediately before the addition of cells and converted to steady state concentration measurements using the sensitivity measured in that day's calibration (see above). The detection limit for these measurements, calculated assuming that the minimum detectable baseline-corrected signal was three times the standard deviation of the baseline, was 100 ± 7 pM. Net superoxide production rates were then calculated as the product of the steady state superoxide concentration and flow rate (final units of pmol h^{-1}). Production rates of superoxide by each population was normalized to the total number of *Trichodesmium* colonies or *Coscinodiscus* cells added to provide colony(or cell)-normalized rates (final units of pmol colony(or cell)$^{-1}$ h^{-1}) (Supporting Information Table S1). Whenever possible, biological replicates were conducted for superoxide measurements using equivalent colony density and light conditions.

Constituents that degrade extracellular superoxide may be present on the cell surface or may have been introduced to the AFSW carrier solution through the cell exudate. To estimate and correct for potential degradation, standard additions of superoxide were performed in a subset of measurements at Station 6 (Supporting Information Table S1). After stable chemiluminescence signals were achieved using the AFSW carrier solution, secondary standards ranging from 3 nM to 60 nM were prepared in an aliquot of identical carrier solution, as described above, and pumped across the cells deposited onto the in-line filter. Standard additions were prepared at concentrations chosen to represent a significant (but not excessive) addition to the cell signal, a factor of no more than three times higher (median). As in calibration experiments, baseline-corrected chemiluminescence data collected over at least 1 min of decay were log-linear. However, in this case, the signal measured immediately before the standard addition was used as the baseline. Time-zero chemiluminescence values were then determined by modeling the log-transformed decay data with pseudo-first order kinetics. The extrapolated chemiluminescence values thus represent the difference in signal due to the added superoxide standard. These were converted to a concentration using the daily calibration factor. These "recovered" concentrations were finally expressed as a percentage of the actual added superoxide concentration (Supporting Information Table S1). Net superoxide production rates were divided by these standard recoveries to generate gross production rates.

To verify that the signal produced by the cells was due to superoxide, SOD (0.8 U mL^{-1}) was added to the buffer at the end of each run. SOD always caused a rapid drop in signal, to a final baseline that was typically below the initial baseline measured before cells were loaded. The difference in the initial and final baselines ($\sim$200 chemiluminescence units) was of the same magnitude as the drop in baseline observed when the same amount of SOD was added to the carrier solution in the absence of cells. The baseline drop reflects either a small, yet non-zero concentration of superoxide in the AFSW carrier solutions and/or (more likely) an effect of SOD on the background chemiluminescence produced by the autooxidation of MCLA (Hansard et al. 2010). To provide

the most conservative value for the superoxide production rates, the higher background baseline was used in biological superoxide production calculations.

Statistical analysis

Differences in superoxide production by *Trichodesmium* (pmol colony^{-1} h^{-1}) among different stations, morphologies (puff, raft, and mixed), light levels (low light vs. dark), and colony numbers were examined in a single linear model of main effects using ANOVA. Separate ANOVA tests were performed to examine the effect of colony number on colony-normalized superoxide production rates by different morphotypes. Post hoc pairwise comparisons were performed where indicated using the Sidak correction.

Results

Superoxide production and decay

A total of 64 superoxide production rates were obtained for 40 different *Trichodesmium* samples collected from the Sargasso Sea (see Supporting Information Table S1). All of the *Trichodesmium* samples analyzed had a chemiluminescence signal well above the aged filtered seawater background (1.3–3.1X) and method detection limit (1.6–58X). The steady-state superoxide concentration maintained by the colonies ranged from 160 pM to 5800 pM, with an average of 1584 ± 967 pM (mean ± SD; $n = 64$). Normalizing the superoxide production rates by colony number resulted in extracellular superoxide production rates that spanned 1.8–69.6 pmol colony^{-1} h^{-1} with a compiled average rate of 11.7 ± 11.9 pmol colony^{-1} h^{-1} (mean ± SD; $n = 64$).

At one station (station 6), superoxide standard additions were conducted to obtain insight into the ability for *Trichodesmium* to concomitantly decay superoxide. Recovery of superoxide spikes ranged from 66% to 100% (average of 85.0% ± 12.7%; $n = 6$). Although we have a limited number of data points, the recoveries did not vary substantially between the puff (89.0% ± 9.5%, $n = 3$) and raft (81.1% ± 16.4%, $n = 3$) morphotypes. These findings indicate that *Trichodesmium* has limited ability and/or need to remove superoxide, consistent with previous observations that removal of *Trichodesmium* colonies from bloom waters by filtering did not significantly decrease superoxide decay rates (Rose et al. 2010). Applying this average recovery value to the compiled average net superoxide production rate gives a slightly higher gross superoxide production rate of 13.5 pmol colony^{-1} h^{-1}. Given the relatively low level of superoxide degradation and that recoveries were not obtained for every sample, only net superoxide production rates will be reported below.

Factors contributing to superoxide production rates

Trichodesmium was collected from eight stations along the cruise transect. A moderate level of inter-station variability was observed, with average rates spanning from 6.3 ± 3.2 pmol colony^{-1} h^{-1} (station 7; $n = 10$) to 23.8 ± 26.1 pmol colony^{-1} h^{-1} (station 4; $n = 8$) (Fig. 2). Overall, *Trichodesmium* produced superoxide at statistically similar rates among all the stations ($F_{6,50} = 1.85$, $p = 0.11$) (Fig. 2). Raft and puff morphologies were present at each station. These morphological types were analyzed independently and/or combined depending on sampling and biomass constraints. The group with the highest level of superoxide production was the mixed raft + puff samples (18.7 ± 20.1 pmol colony^{-1} h^{-1}), followed by puffs (10.8 ± 8.1 pmol colony^{-1} h^{-1}), and finally, rafts (8.7 ± 7.2 pmol colony^{-1} h^{-1}) (Fig. 3). Morphology did not significantly influence superoxide production overall ($F_{2,50} = 0.45$, $p = 0.64$) (Fig. 3A).

Some samples were analyzed in the dark (0 μmol photon m^{-2} s^{-1}) and under low light (~50 μmol photon m^{-2} s^{-1}). In the light, *Trichodesmium* produced superoxide nearly 70% faster than in the dark, which was a statistically significant difference ($F_{1,50} = 10.70$, $p < 0.01$) (Fig. 3B). However, this light effect was only observed for the raft morphology and mixed raft + puff samples, not puffs (Figs. 4, 5). The increase in superoxide production rates by rafts on introduction of light ranged from 24% to 92%, with an average of 49.3% ± 7.6% (mean ± SEM). This light effect is evident from the real time superoxide signals obtained for the raft colonies under fluctuating light conditions (see, for example, Fig. 5B), which are directly proportional to steady state superoxide levels produced by *Trichodesmium*. Within seconds of introducing low light levels (~50 μmol photon m^{-2} s^{-1}), an increase was observed in the chemiluminescent signal (Fig. 5B). Turning off the light lead to a rapid decline back to the original chemiluminescent level or below. This pattern repeated under fluctuating light and dark conditions. Mixed communities behaved similar to the raft morphotypes in that production rates increased in the presence of low light (Fig. 4), although this increase was only statistically relevant ($p < 0.05$) at low colony densities (see Fig. 6C,E). Superoxide production in the absence of *Trichodesmium* (solely 0.2 μm filtered seawater) did not change in response to light, indicating that the observed change in superoxide production in the presence of *Trichodesmium* was due to either a direct biological response or photochemical reaction with a *Trichodesmium*-derived exudate (not a photochemical reaction in the AFSW solution).

Lastly, the number of *Trichodesmium* colonies added to the filter was varied (from 10 to 40 colonies), to examine possible cell density effects on superoxide production. When considering all the measurements together (not differentiating by morphology), colony-normalized rates of superoxide production significantly decreased with increasing colony number ($F_{3,50} = 13.75$, $p < 0.01$), even though the lowest colony abundance level ($n = 10$) had a high degree of variability (Fig. 3C). On closer inspection, colony number had different effects on raft vs. puff morphologies, both in terms of steady-state superoxide levels (Fig. 6A–C) and superoxide

production rates (Fig. 6D–F; Supporting Information Fig. S2). For rafts, steady-state superoxide concentrations (Fig. 6A-C) and production rates (Supporting Information Fig. S2) tended to increase with increasing colony number, whereas the opposite trend was evident for puffs and mixed colonies. These trends, however, were not significant ($p > 0.05$). Normalizing these superoxide production rates to colony number revealed further differences between morphotypes. For rafts, colony-normalized superoxide production rates did not vary with colony abundance in the light ($F_{1,10} = 0.32$, $p = 0.58$) or dark ($F_{2,10} = 0.23$, $p = 0.80$) (Fig. 6D). In stark contrast, however, the rate of superoxide production per colony significantly decreased with colony density for puffs (Light: $F_{2,12} = 8.37$, $p = 0.01$; Dark: $F_{2,6} = 18.16$, $p < 0.01$) and mixed raft/puff colonies (Dark: $F_{2,5} = 25.62$, $p < 0.01$) (Fig. 6E,F). There was no sufficient replication to statistically examine the effect of colony number on superoxide production by mixed colonies in the light.

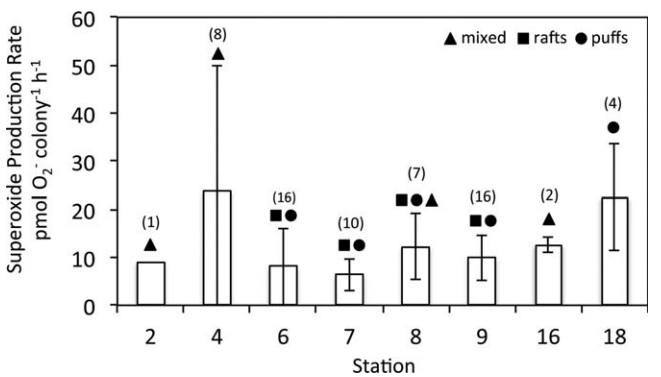

Fig. 2. Compilation of 64 colony-normalized superoxide production rates in pmol colony^{-1} h^{-1} measured for *Trichodesmium* colonies collected at eight stations (as shown in Fig. 1). Duration of the steady-state superoxide signal measured ranged from 24 s to 250 s with an average of 100 s (see Supporting Information Table S1). Symbols above bars indicate the morphological composition of the colonies analyzed at each station. Numbers above the symbols indicate the number of samples analyzed and included in the data shown.

Superoxide production by a co-inhabitant of the planktonic community

At station 14 and 16, the large solitary diatom *Coscinodiscus* was abundant in plankton tow samples, along with *Trichodesmium*. Constraints on reagent availability at the end of the cruise, however, precluded a thorough analysis of superoxide production by this organism. Steady-state levels of extracellular superoxide from *Coscinodiscus* ranged from ~3.2 nM (station 14; $n = 2$) to 0.6 nM (station 16; $n = 1$) (Supporting Information Table S1). Only one *Coscinodiscus* sample was analyzed at station 16, which produced superoxide at a rate of 0.9 fmol cell^{-1} h^{-1} (ca. 75,000 cells). At station 14, two *Coscinodiscus* samples had an average superoxide production rate of 13.7 ± 0.5 fmol cell^{-1} h^{-1} (ca. 27,000 cells each). One of these samples was run in the dark (13.4 fmol cell^{-1} h^{-1}) and one in the light (14.0 fmol cell^{-1} h^{-1}), suggesting a negligible influence of low light (~50 μmol photon m^{-2} s^{-1}) on superoxide production by this diatom. Although the cell numbers used for sample analysis at station 14 were nearly three times lower than at station 16, the measured superoxide production rate was substantially higher, yet with this small number of measurements, interpretation is limited. A consortium containing *Coscinodiscus* (ca. 6000 cells) and *Trichodesmium* (15 puff and 2 raft colonies) had a substantially higher superoxide production rate of 13.2 pmol organism^{-1} h^{-1} compared with the diatom in isolation, rates that are reflective of *Trichodesmium*'s overriding contribution. Superoxide decay by *Coscinodiscus* at Station 16 was stronger (31% superoxide recovery) than that observed for the *Trichodesmium* colonies and well above the decay measured by the consortium of *Coscinodiscus* and *Trichodesmium* (100% recovery).

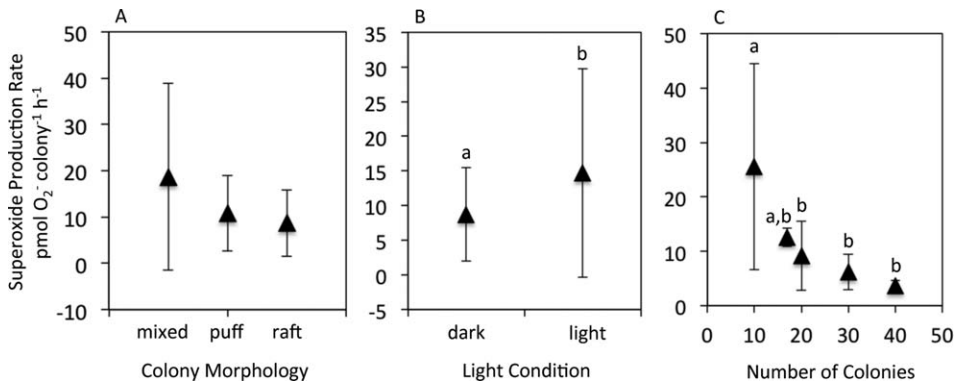

Fig. 3. Colony-normalized superoxide production rates grouped by colony morphology (**A**), light conditions (**B**), and colony number (**C**). Morphotypes included puff ($n = 25$), raft ($n = 25$) or mixed puff and raft ($n = 14$), light conditions were either dark ($n = 32$) or low light ($n = 32$), and colony numbers were 10 ($n = 13$), 17 ($n = 2$), 20 ($n = 33$), 30 ($n = 12$) or 40 ($n = 4$). PAR measurements for the dark and light conditions were 0 μmol photon m^{-2} s^{-1} and ~ 50 μmol photon m^{-2} s^{-1}, respectively. Pairwise comparisons are significant ($p < 0.05$) only if indicated by different letters.

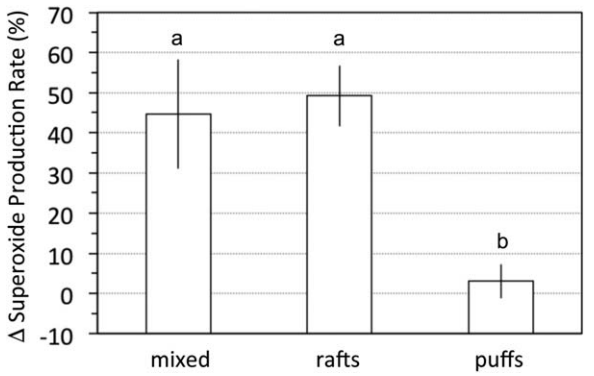

Fig. 4. Change in superoxide production rates for mixed ($n = 3$), raft ($n = 8$), and puff ($n = 6$) colonies in the light relative to the dark. Comparison is restricted to samples where both light and dark measurements were made on the same sample in-line (not between different samples) (see Supporting Information Table S1). Pairwise comparisons that are significant ($p < 0.05$) are indicated by different letters.

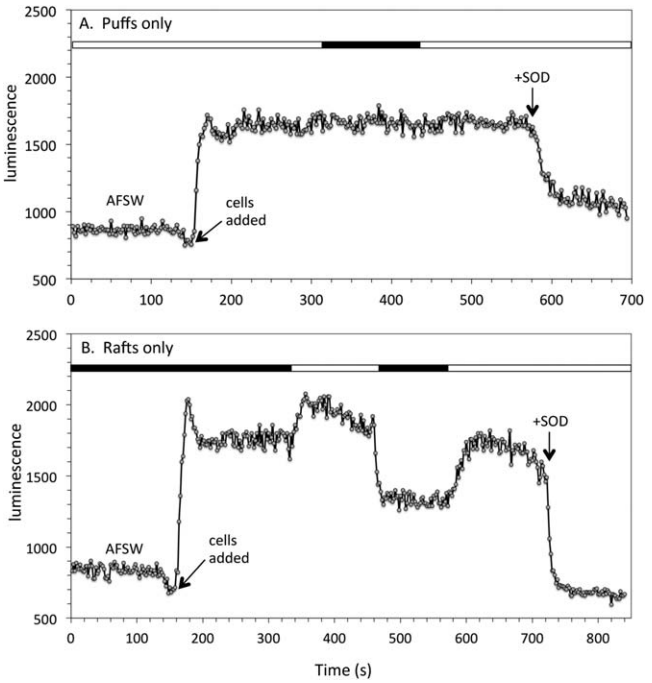

Fig. 5. Representative FeLume chemiluminescent profile for puff (**A**) and raft (**B**) colonies under fluctuating light and dark conditions. The number of colonies analyzed for the puff and raft measurement was 20 and 30, respectively. Bar on the top of the profiles indicates the absence (black) or presence (white) of light. AFSW, aged, filtered seawater; SOD, superoxide dismutase.

Discussion

Here, we report substantial rates of extracellular superoxide production by the cyanobacterium *Trichodesmium* and the solitary diatom *Coscinodiscus* harvested from the Sargasso Sea. To the best of our knowledge, superoxide production rates for diatoms are currently limited to three species of *Thalassiosira—T. weissflogii*, *T. pseudonana*, and *T. oceanica*, where net superoxide production rates span 0.2–1.4 fmol cell^{-1} h^{-1} (Kustka et al. 2005; Rose et al. 2008b; Milne et al. 2009; Schneider et al., In Press). Thus, superoxide production rates by *Coscinodiscus* are comparable to and on the higher end of recorded rates for other diatoms. Taking into consideration however the significantly higher surface area of *Coscinodiscus* (average of ~50,000 μm^2 cell^{-1}) compared with *Thalassiosira* (~51–460 μm^2 cell^{-1}), the average surface area normalized rate for *Coscinodiscus* (0.19 ± 0.14 amol μm^{-1} h^{-1}) is substantially lower than those for *T. weissflogii* (1.8 ± 0.8 amol μm^{-2} h^{-1}) and *T. pseudonana* (8.0 ± 1.5 amol μm^{-2} h^{-1}) (Rose et al. 2008).

The diazotroph *Trichodesmium* consistently produced high rates of extracellular superoxide (1.8–69.6 pmol colony^{-1} h^{-1}). These superoxide production rates are consistent with measured rates of 1.59 ± 0.09 pmol trichome^{-1} h^{-1} by laboratory cultures of *Trichodesmium erythraeum* IMS101 (Godrant et al. 2009). This laboratory culture was present as free filaments (trichomes) and not assembled as colonies, as in our natural *Trichodesmium* colonies. For the sake of comparison, if we assume an average of 150 trichomes per colony (Letelier and Karl 1996; Carpenter et al. 2004), the average trichome normalized superoxide production rate by our natural *Trichodesmium* colonies was 0.08 ± 0.08 pmol trichome^{-1} h^{-1}. Although our rates are 20 times lower, these results are surprisingly aligned considering the difference in *Trichodesmium* morphotypes analyzed and that Godrant et al (2009) used a different method for superoxide detection (consisting of incubation of *Trichodesmium* directly within the chemiluminescent reagent in microplates rather than a flow through injection as employed here). In particular, the microplate method measures gross superoxide production, whereas the flow through method provides net production (unless corrected for decay, which we did not do here).

These results are also consistent with previous observations of superoxide production in natural *Trichodesmium* blooms. Quasi-steady-state superoxide levels within *Trichodesmium* blooms in the Great Barrier Reef (GBR) lagoon averaged 711 ± 550 pM (Rose et al. 2010). The authors calculated a corresponding net superoxide production rate within the *Trichodesmium* bloom of 7 ± 4 pM s^{-1} (or 25,200 pM h^{-1}) by extrapolation of the decay kinetics of 0.2 μm filtered bloom water (reported rates were not normalized to colony number) (Rose et al. 2010). Taking into account our average measured extracellular superoxide production rate by *Trichodesmium* (11.7 pmol colony^{-1} h^{-1}), a *Trichodesmium* density of ~2100 colonies per liter would be required to produce the calculated superoxide production rate within the GBR lagoon bloom. These densities are not realistic as a maximum reported value for *Trichodesmium* abundance in blooms within this region is ~27 colonies per liter (~4000 filaments per liter observed and assuming ~150 filaments per colony) (Carpenter et al. 1992). These findings instead point to other controls on in situ

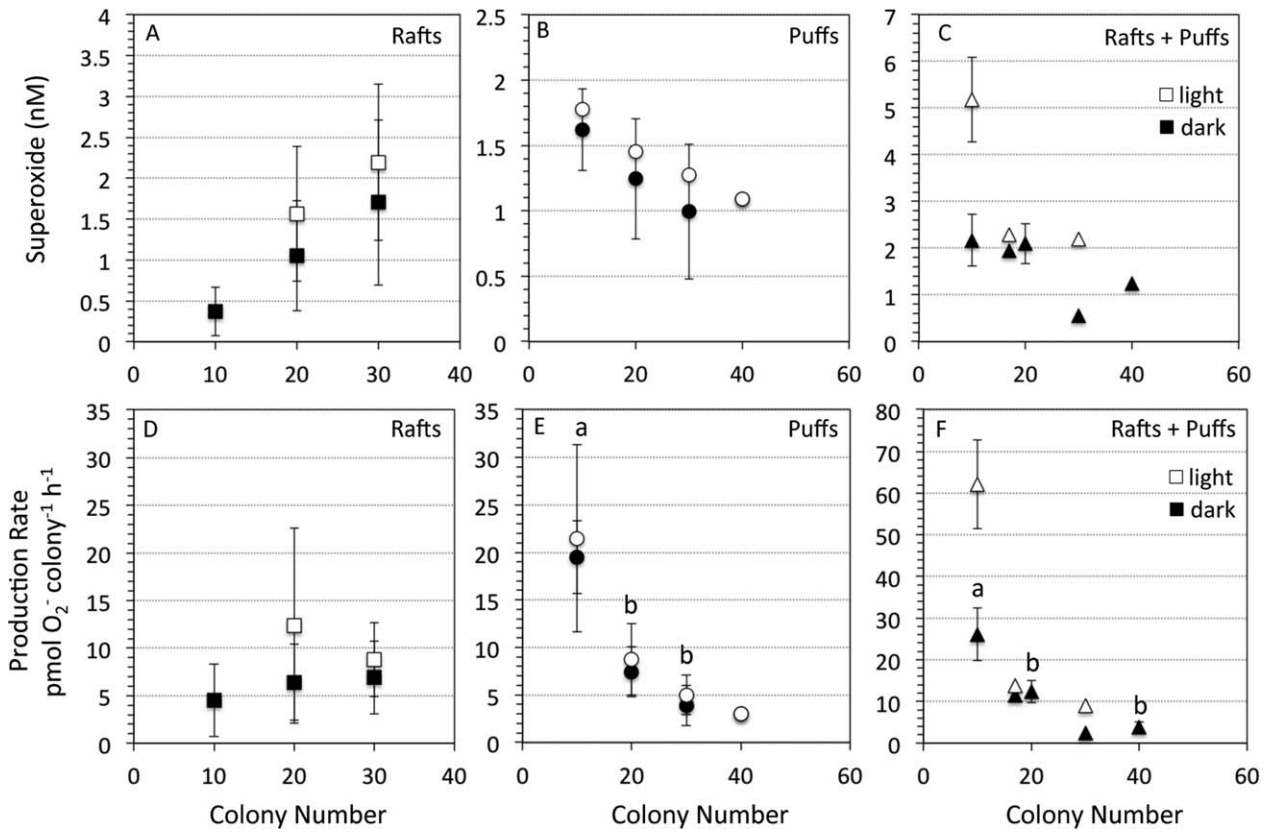

Fig. 6. Superoxide steady-state concentrations (**A**–**C**) and colony normalized production rates (**D**–**F**) as a function of the number of colonies used in the superoxide measurement. Pairwise comparisons between different colony numbers for the same light condition are indicated (E, F). These pairwise comparisions are significant ($p < 0.05$) only if indicated by different letters. Letters correspond to the light and dark (for E) and dark only (for F) datasets.

superoxide production rates by *Trichodesmium* and/or contributions by other phytoplankton and bacteria within coastal bloom waters (Rose et al. 2010). If we consider typical *Trichodesmium* densities during non-bloom conditions in the Sargasso Sea of approximately 0.8 colonies per liter (Olson et al. 2015) and our average extracellular superoxide production rate (11.7 pmol colony^{-1} h^{-1}), then *Trichodesmium* contributes superoxide to the surface Sargasso Sea waters at a rate of approximately 9.4 pM per hour. Nevertheless, as evident by the mixed and puff measurements (Fig. 6, Supporting Information Fig. S2), superoxide production rates will be higher at lower cell densities under some conditions and therefore this extrapolation may underestimate in situ production rates within *Trichodesmium*-bearing waters. Within oligotrophic regions of the ocean, *Trichodesmium* may therefore be a significant and possibly primary source of superoxide to surface waters, even during non-bloom conditions. These levels of superoxide will no doubt influence the surrounding redox conditions through interactions with metals and carbon in the surface waters.

Making predictions on in situ *Trichodesmium* contributions to superoxide levels, however, will need to take into consideration the morphology of the colonies. In particular, colony density and light had a variable impact on extracellular superoxide production depending on *Trichodesmium* morphology. The physiological health of the *Trichodesmium* colonies, as estimated by the maximum photochemical quantum yield of photosystem II (F_v/F_m), did not vary significantly between the different sites or for puff vs. raft morphologies (see Supporting Information Table S2). The basis for this morphological-dependent influence on superoxide production is currently unknown, but may point to fundamental differences in the biochemical pathways responsible for extracellular superoxide production by these two morphotypes and/or functional differences in the bacterial epibiont community associated with the *Trichodesmium* colonies.

First, the higher superoxide levels generated in the presence of light for the raft morphotypes may suggest a link to photosynthetic activity in superoxide production for these organisms but not for puffs, despite their similar physiological status and photosynthetic capacity (as in F_v/F_m—see Supporting Information Table S2). Light enhanced superoxide production has been observed previously for some phytoplankton,

including the red tide raphidophyte *C. marina* (Marshall et al. 2002), the red tide dinoflagellate *Cochlodinium polykrikoides* (Kim et al. 1999), the coral symbiont *Symbiodinium* sp. (Saragosti et al. 2010), and more recently various *Thalassiosira* species (Schneider et al., In Press). Further, addition of the photosynthesis inhibitor DCMU (3-(3,4-dichlorophenyl)−1,1-dimethyl sulfoxide) has been shown to decrease superoxide production in *C. marina* cultures (Marshall et al. 2002), as well as natural seawater samples collected from outside and within *Trichodesmium* blooms (Rose et al. 2010). While electron transport during photosynthetic activity could lead to increased intracellular superoxide levels, superoxide has limited ability to cross membranes and lipid bilayers (Korshunov and Imlay 2002) and will therefore have a negligible influence on the extracellular signal (Rose 2012). Instead, an indirect link between photosynthetic activity and extracellular superoxide production is more likely operative. DCMU is a membrane permeable compound that disrupts electron flow at the plastoquinone site of photosystem II, leading to inhibited production of NADPH. Within eukaryotes, NADPH is a source of reducing equivalents within the cell that can act to shuttle electrons through transmembrane oxidoreductase enzymes, such as NADPH oxidases, to oxygen outside the cell (Bedard et al. 2007), as has been clearly demonstrated for fungi (Aguirre et al. 2005) and suggested for *Chattonella* (Kawano et al. 1996). In the *Trichodesmium* raft colonies, a similar mechanism could be operative, where light increased NADPH levels within the cell that subsequently increased electron transfer to presently unknown outer-membrane and/or transmembrane enzymes involved in extracellular superoxide production.

While light did not influence puff colonies, colony number had a substantial influence on superoxide production on this morphotype, which was not seen for the raft colonies. In particular, colony-normalized superoxide production rates were inversely related to colony density for puff colonies. These results are similar to our previous investigations of cell density dependence of superoxide production by heterotrophic bacteria (Diaz et al. 2013). For example, the Alphaproteobacterium *Ruegaria* sp. TM1040 and Gammaproteobacterium *Vibrio* sp. A535 both demonstrated a decline in cell-normalized superoxide production rates with increasing cell density (Supporting Information Fig. S3; Diaz et al. 2013). Similarly, a complex relationship was previously observed between cell density and the superoxide produced per cell for *C. marina* and the prymnesiophyte alga *Prymnesium parvum* (Marshall et al. 2005). Below 10,000 *C. marina* cells, cell-normalized superoxide production rates increased with cell density. However, above this density, an inverse relationship was observed for cell density and superoxide produced per cell. Furthermore, serial dilution of both medium- and high-density *C. marina* cultures resulted in significantly increased cell normalized superoxide production levels and production rates following 1 h of incubation (Marshall et al. 2005).

Overall, results suggest that the rate of net superoxide production is regulated by puff morphotypes as a function of cell density. The higher rates of superoxide production per colony at lower densities could also suggest that superoxide is involved in cell growth. Indeed, extracellular superoxide is involved in cell viability and proliferation among toxic phytoplankton and pathogenic bacteria (Oda et al. 1995; Saran 2003; Buetler et al. 2004). For instance, superoxide production is tightly regulated during growth of some bacterial strains (Carlioz and Touati 1986; Storz et al. 1987). Further, on entering stationary phase, some bacteria start expressing a periplasmic SOD that is attached to the outer surface of the membrane (Benov and Fridovich 1994). Similarly, within cultures of the toxic raphidophyte *C. marina*, superoxide production was highest during growth with concentrations decreasing by 80% during stationary phase (Oda et al. 1995). Further, SOD strongly inhibited growth of *C. marina* in a concentration-dependent manner, resulting in a lack of asexual division and the conclusion that superoxide may function as an autocrine growth factor (Oda et al. 1995). While the mechanisms of growth stimulation in phytoplankton have not been resolved, superoxide is widely recognized for its essential role in cell signaling and growth in fungi, plants and animals (Saran 2003; Buetler et al. 2004). Within fungal and mammalian cells, superoxide has been linked to growth as a local signaling molecule where it serves to modulate membrane lipid structure and influence cell responsiveness to growth factors (Saran 2003; Buetler et al. 2004). Although speculative at this point in time, the higher superoxide levels and production rates at lower colony densities within the *Trichodesmium* puff colonies could point to a similar role for superoxide in aiding cell growth and proliferation. This would assume that the *Trichodesmium* colonies were physiologically active and in growth phase within the lab incubations, which is supported by a parallel study showing phosphorus uptake by colonies collected at these stations (Van Mooy et al. 2015).

Thus, in *Trichodesmium*, controls on superoxide production appear to vary with colony morphology, which may reflect differences in the physiology of the puff and raft morphotypes. Why similar light- and colony density-dependent mechanisms are not operative within the puff and raft morphotypes, however, are not obvious. Nevertheless, while *Trichodesmium* forms a range of morphologies in culture and within natural systems, the reasons for and consequences of assembling their trichomes into various morphotypes is unclear. Some evidence suggests that specific morphotypes may provide different physiological advantages. For instance, puffs may be more efficient at iron(III) uptake than tufts (Achilles et al. 2003), as only puff morphologies have the ability to mediate the dissolution of iron-containing dust particles to support the acquisition of iron (Rubin et al. 2011). Puff and bow-tie colonies of *Trichodesmium* have also been found to have significantly higher (10-fold to 100-fold)

alkaline phosphatase (AP) activity than tuft colonies obtained from the same surface waters in the Red Sea (Stihl et al. 2001). The authors posed that this morphology-based variation pointed to differences in the phosphorus status between the different morphotypes. Similarly, puff and tuft morphotypes from the western Central and western South Atlantic showed different chlorophyll (Chl) *a*-normalized N_2 fixation rates and AP activities, suggesting that these two morphotypes may respond differently to phosphorous stress (Webb et al. 2007). Further, the puff morphotypes typically had a higher Chl *a* content, suggesting that the puff forms may have adapted to live at depth, where light levels are lower. A lower Chl *a* content within puff morphotypes could also possibly explain a diminished response to light and corresponding lack of light enhanced superoxide production, in contrast to the raft communities.

Another plausible explanation could be that differences in the epibiont community hosted by *Trichodesmium* may also contribute to the observed variations in superoxide production. *Trichodesmium* harbors an abundant microbial community, including bacteria, diatoms, cyanobacteria and viruses (Paerl et al. 1989; Sheridan et al. 2002; Hmelo et al. 2012). Previous investigations of puff and tuft (i.e., raft) colonies from the Sargasso Sea revealed that the *Trichodesmium*-hosted microbial communities are distinctly different than the surrounding seawater suggesting that *Trichodesmium* selects for a specific consortial community (Hmelo et al. 2012). This epibiont community varied also for puff vs. tuft morphologies (Hmelo et al. 2012). Of particular interest here is that the tuft (raft) colonies contained other cyanobacterial members, which was not observed for the puff colonies. Cyanobacteria were not observed, however, in a recent investigation of the epibiont communities harbored on *Trichodesmium* at stations in the Sargasso Sea near our transect (Dyhrman, unpubl. data). A lack of cyanobacteria however does not rule out other light-responsive epibionts, particularly bacteria that contain proteorhodopsin. Assuming that the *Trichodesmium* colonies analyzed in our study also harbored functionally distinct microbial consortia, these epibionts could in theory influence superoxide fluxes through their contributions to superoxide production and/or decay. Other phototrophic superoxide contributions within the raft colonies could, for instance, help to explain why light influenced raft communities (likely a photosynthetic response) but not puff communities.

Colony density controls on superoxide production rates could also stem from the epibiont community. While we have previously observed an inverse relationship between cell density and superoxide production for heterotrophic bacteria (see for example, Supporting Information Fig. S3), there is not enough data currently available to predict how superoxide production rates vary with cell density as a function of bacterial species. Nevertheless, we have previously shown a wide range of superoxide production rates by heterotrophic bacteria (Diaz et al. 2013), and our current research points to different enzymatic processes responsible for this production (Hansel, unpubl. data) suggesting that superoxide fluxes will vary with bacterial community composition.

Thus, at present it is difficult to specifically link light- and cell density-based effects on superoxide production as a function of the epibiont abundance and species composition. If these epibiont communities are contributing to superoxide fluxes, then a key question is whether the establishment of these different communities is fortuitous or intentional to specifically manipulate superoxide levels for the benefit of the host *Trichodesmium*. Teasing out the relative role of the *Trichodesmium* host vs. their epibionts on the patterns of superoxide production we observed here will require further targeted investigations of cultures, both mixed and axenic, under controlled laboratory conditions. Regardless of the mechanistic underpinnings, these findings point to complex physiological and ecological influences on superoxide dynamics in *Trichodesmium* that require further targeted exploration.

References

Achilles, K. M., T. M. Church, S. W. Wilhelm, G. W. Luther Iii, and D. A. Hutchins. 2003. Bioavailability of iron to *Trichodesmium* colonies in the western subtropical Atlantic Ocean. Limnol. Oceanogr. **48**: 2250–2255. doi:10.4319/lo.2003.48.6.2250

Aguirre, J., M. Rios-Momberg, D. Hewitt, and W. Hansberg. 2005. Reactive oxygen species and development in microbial eukaryotes. Trends Microb. **13**: 111–118. doi:10.1016/j.tim.2005.01.007

Archibald, F. S., and I. Fridovich. 1982. The scavenging of superoxide radical by manganous complexes: In Vitro. Arch Biochem. Biophys. **214**: 452–463. doi:10.1016/0003-9861(82)90049-2

Bedard, K., B. Lardy, and K.-H. Krause. 2007. NOX family NADPH oxidases: Not just in mammals. Biochimie **89**: 1107–1112. doi:10.1016/j.biochi.2007.01.012

Benov, L. T., and I. Fridovich. 1994. *Escherichia coli* expresses a copper- and zinc-containing superoxide dismutase. J. Biol. Chem. **269**: 25310–25314.

Berman-Frank, I., K. Bidle, L. Haramaty, and P. G. Falkowski. 2004. The demise of the marine cyanobacterium, *Trichodesmium* spp., via an autocatalyzed cell death pathway. Limnol. Oceanogr. **49**: 997–1005. doi:10.4319/lo.2004.49.4.0997

Berman-Frank, I., G. Rosenberg, O. Levitan, L. Haramaty, and X. Marl. 2007. Coupling between autocatalytic cell death and transparent exopolymeric particle production in the marine cyanobacterium *Trichodesmium*. Environ. Microbiol. **9**: 1415–1422. doi:10.1111/j.1462-2920.2007.01257.x

Bielski, B. H. J., D. E. Cebelli, and R. L. Arudi. 1985. Reactivity of HO_2/O_2^- radicals in aqueous solution. J. Phys. Chem. Ref. Data **14**: 1041–1100. doi:10.1063/1.555739

Buetler, T. M., A. Krauskopf, and U. T. Ruegg. 2004. Role of superoxide as a signaling molecule. Physiology **19**: 120–123. doi:10.1152/nips.01514.2003

Capone, D. G., J. P. Zehr, H. W. Paerl, B. Bergman, and E. J. Carpenter. 1997. *Trichodesmium*, a globally significant marine cyanobacterium. Science **276**: 1221–1229. doi:10.1126/science.276.5316.1221

Carlioz, A., and D. Touati. 1986. Isolation of SOD mutants in *Escherichia coli*: Is SOD necessary for aerobic life? EMBO J. **5**: 623–630.

Carpenter, E. J., D. G. Capone, and J. G. Rueter. 1992. Marine pelagic cyanobacteria: Trichodesmium and other diazotrophs. Springer Science & Business Media.

Carpenter, E. J., A. Subramaniam, and D. G. Capone. 2004. Biomass and primary productivity of the cyanobacterium *Trichodesmium* spp. in the tropical N Atlantic ocean. Deep-Sea Res. I **51**: 173–203. doi:10.1016/j.dsr.2003.10.006

Diaz, J., C. M. Hansel, B. M. Voelker, C. M. Mendes, P. F. Andeer, and T. Zhang. 2013. Widespread production of extracellular superoxide by marine heterotrophic bacteria. Science **340**: 1223–1226. doi:10.1126/science.1237331

Fridovich, I. 1998. Oxygen toxicity: A radical explanation. J. Exp. Biol. **201**: 1203–1209.

Godrant, A., A. L. Rose, G. Sarthou, and T. D. Waite. 2009. New method for the determination of extracellular production of superoxide by marine phytoplankton using the chemiluminescence probes MCLA and red--CLA. Limnol. Oceanogr. **7**: 682–692. doi:10.4319/lom.2009.7.682

Hansard, S. P., A. W. Vermilyea, and B. M. Voelker. 2010. Measurements of superoxide radical concentration and decay kinetics in the Gulf of Alaska. Deep-Sea Res. I **57**: 1111–1119. doi:10.1016/j.dsr.2010.05.007

Hansard, S. P., H. D. Easter, and B. M. Voelker. 2011. Rapid reaction of nanomolar Mn(II) with superoxide radical in seawater and simulated freshwater. Environ. Sci. Technol. **45**: 2811–2817. doi:10.1021/es104014s

Hansel, C. M., C. A. Zeiner, C. M. Santelli, and S. M. Webb. 2012. Mn(II) oxidation linked to superoxide production during asexual reproduction in an Ascomycete fungi. Proc. Natl. Acad. Sci. USA **109**: 12621–12625. doi:10.1073/pnas.1203885109

Hmelo, L. R., B. A. S. Van Mooy, and T. J. Mincer. 2012. Characterization of bacterial epibionts on the cyanobacterium *Trichodesmium*. Aquat. Microb. Ecol. **67**: 1–14. doi:10.3354/ame01571

Hynes, A. M., E. A. Webb, S. C. Doney, and J. B. Waterbury. 2012. Comparison of cultured *Trichodesmium* (Cyanophyceae) with species characterized from the field. J. Phycol. **48**: 196–210. doi:10.1111/j.1529-8817.2011.01096.x

Karthik, R., M. Arun Kumar, S. Sai Elangovan, R. Siva Sankar, and G. Padmavati. 2012. Phytoplankton abundance and diversity in the coastal waters of Port Blair, South Andaman Island in relation to environmental variables. J. Mar. Biol. Oceanogr. **1**: 2. doi:10.1186/2046-9063-8-20

Kawano, I., T. Oda, A. Ishimatsu, and T. Muramatsu. 1996. Inhibitory effects of the iron chelator Desferrioxamine (Desferal) on the generation of activated oxygen spcies of *Chattonella marina*. Mar. Biol. **126**: 765–771. doi:10.1007/BF00351343

Kim, C. S., S. G. Lee, C. K. Lee, H. G. Kim, and J. Jung. 1999. Reactive oxygen species as causative agents in the ichthyotoxicity of the red tide dinoflagellate *Cochlodinium polykrikoides*. J. Plankton Res. **21**: 2105–2115. doi:10.1093/plankt/21.11.2105

Kim, D., and others. 2000. Mechanism of superoxide anion generation in the toxic red tide phytoplankton *Chattonella marina*: Possible involvement of NAD(P)H oxidase. Biochim. Biophys. Acta Gen. Sub. **1524**: 220–227. doi:10.1016/S0304-4165(00)00161-6

Korshunov, S. S., and J. A. Imlay. 2002. A potential role for periplasmic superoxide dismutase in blocking the penetration of external superoxide into the cytosol of Gram-negative bacteria. Mol. Microbiol. **43**: 95–106. doi:10.1046/j.1365-2958.2002.02719.x

Kustka, A. B., Y. Shaked, A. J. Milligan, D. W. King, and F. M. M. Morel. 2005. Extracellular production of superoxide by marine diatoms: Contrasting effects on iron redox chemistry and bioavailability. Limnol. Oceanogr. **50**: 1172–1180. doi:10.4319/lo.2005.50.4.1172

Learman, D. R., B. M. Voelker, A. I. Vazquez-Rodriguez, and C. M. Hansel. 2011. Formation of manganese oxides by bacterially generated superoxide. Nat. Geosci. **4**: 95–98. doi:10.1038/ngeo1055

Learman, D. R., B. M. Voelker, A. S. Madden, and C. M. Hansel. 2013. Constraints on superoxide mediated formation of manganese oxides. Front. Microbiol. **4**: 1–11. doi:10.3389/fmicb.2013.00262

Letelier, R. M., and D. M. Karl. 1996. Role of *Trichodesmium* spp. in the productivity of the subtropical Norh Pacific Ocean. Mar. Ecol. Prog. Ser. **133**: 263–273. doi:10.3354/meps133263

Li, H.-P., and others. 2014. Superoxide production by a manganese-oxidizing bacterium facilitates iodide oxidation. Appl. Environ. Microbiol. **80**: 2693–2699. doi:10.1128/AEM.00400-14

Marshall, J. A., M. Hovenden, T. Oda, and G. M. Hallegraeff. 2002. Photosynthesis does influence superoxide production in the ichthyotoxic alga *Chatonella marina* (Raphidophyceae). J. Plankton Res. **24**: 1231–1236. doi:10.1093/plankt/24.11.1231

Marshall, J. A., T. Ross, S. Pyecroft, and G. Hallegraeff. 2005. Superoxide production by marine microalgae - II. Towards understanding ecological consequences and possible functions. Mar. Biol. **147**: 541–549. doi:10.1007/s00227-005-1597-6

Millero, F. J., and S. Sotolongo. 1989. The oxidation of Fe(II) with H2O2 in seawater. Geochim. Cosmochim. Acta **53**: 1867–1873. doi:10.1016/0016-7037(89)90307-4

Milne, A., M. S. Davey, P. J. Worsfold, E. P. Achterberg, and A. R. Taylor. 2009. Real-time detection of reactive oxygen

species generation by marine phytoplankton using flow injection-chemiluminescence. Limnol. Oceanogr.: Methods **7**: 706–715. doi:10.4319/lom.2009.7.706

Moffett, J. W., and R. G. Zika. 1987. Reaction kinetics of hydrogen peroxide with copper and iron in seawater. Environ. Sci. Technol. **21**: 804–810. doi:10.1021/es00162a012

Oda, T., and others. 1992. Hydroxyl radical generation by red time algae. Arch. Biochem. Biophys. **294**: 38–43. doi:10.1016/0003-9861(92)90133-H

Oda, T., J. Moritomi, I. Kawano, S. Hamaguchi, A. Ishimatsu, and T. Muramatsu. 1995. Catalase- and superoxide dismutase-induced morphological changes and growth inhibition in the red tide phytoplankton *Chattonella marina*. Biosci. Biotechnol. Biochem. **59**: 2044–2048. doi:10.1271/bbb.59.2044

Olson, E. M., D. J. Mcgillicuddy, G. R. Flierl, C. S. Davis, S. T. Dyhrman, and J. B. Waterbury. 2015. Mesoscale eddies and *Trichodesmium* spp. distributions in the southwestern North Atlantic. J. Geophys. Res. Oceans **120**: 4129–4150. doi:10.1002/2015JC010728

Paerl, H. W., B. M. Bebout, and L. E. Prufert. 1989. Bacterial associations with marine *Oscillatoria* sp. (*Trichodesmium* sp.) populations: Ecophysiological implications. J. Phycol. **25**: 773–784. doi:10.1111/j.0022-3646.1989.00773.x

Roe, K. L., and K. A. Barbeau. 2014. Uptake mechanisms for inorganic iron and ferric citrate in *Trichodesmium erythraeum* IMS101. Metallomics **6**: 2042–2051. doi:10.1039/C4MT00026A

Rose, A. L. 2012. The influence of extracellular superoxide on iron redox chemistry and bioavailability to aquatic microorganisms. Front. Microb. Chem. **3**: 1–21. doi:10.3389/fmicb.2012.00124

Rose, A. L., T. P. Salmon, T. Lukondeh, B. A. Neilan, and T. D. Waite. 2005. Use of superoxide as an electron shuttle for iron acquisition by the marine cyanobacterium *Lyngbya majuscula*. Environ. Sci. Technol. **39**: 3708–3715. doi:10.1021/es048766c

Rose, A. L., J. W. Moffett, and T. D. Waite. 2008a. Determination of superoxide in seawater using 2-methyl-6-(4-methoxyphenyl)−3,7-dihydroimidazol(1,2-a)pyrazin-3(7H)-one chemiluminescence. Anal. Chem. **80**: 1215–1227. doi:10.1021/ac7018975

Rose, A. L., E. A. Webb, T. D. Waite, and J. W. Moffett. 2008b. Measurement and implications of nonphotochemically generated superoxide in the equatorial Pacific Ocean. Environ. Sci. Technol. **42**: 2387–2393.

Rose, A. L., A. Godrant, M. Furnas, and T. D. Waite. 2010. Dynamics of nonphotochemical superoxide production and decay in the Great Barrier Reef lagoon. Limnol. Oceanogr. **55**: 1521–1536. doi:10.4319/lo.2010.55.4.1521

Rubin, M., I. Berman-Frank, and Y. Shaked. 2011. Dust- and mineral-iron utilization by the marine dinitrogen-fixer *Trichodesmium*. Nat. Geosci. **4**: 529–534. doi:10.1038/ngeo1181

Saragosti, E., D. Tchernov, A. Katsir, and Y. Shaked. 2010. Extracellular production and degradation of superoxide in the coral *Stylophora pistillata* and cultured *Symbiodinium*. PLoS ONE **5**: e12508. doi:10.1371/journal.pone.0012508

Saran, M. 2003. To what end does nature produce superoxide? NADPH oxidase as an autocrine modifier of membrane phospholipids generating paracrine lipid messengers. Free Rad. Res. **37**: 1045–1059.

Schneider, R. J., K. L. Roe, C. M. Hansel, B. M. Voelker. In Press. Species-level variability in extracellular production rates of reactive oxygen species by diatoms. Frontiers in Marine Biogeochemistry doi:10.3389/fchem.2016.00005

Sheridan, C. C., D. K. Steinberg, and G. W. Kling. 2002. The microbial and metazoan community associated with colonies of *Trichodesmium* spp.: A quantitative survey. J. Plankton Res. **24**: 913–922. doi:10.1093/plankt/24.9.913

Stihl, A., U. Sommer, and A. F. Post. 2001. Alkaline phosphatase activities among populations of the colony-forming diazotrophic cyanobacterium *Trichodesmium* spp. (cyanobacteria) in the Red Sea. J. Phycol. **37**: 310–317. doi:10.1046/j.1529-8817.2001.037002310.x

Storz, G., M. F. Christman, H. Sies, and B. N. Ames. 1987. Spontaneous mutagenesis and oxidative damage to DNA in *Salmonella typhimurium*. Proc. Natl. Acad. Sci. USA **84**: 8917–8921. doi:10.1073/pnas.84.24.8917

Tang, Y., C. A. Zeiner, C. M. Santelli, and C. M. Hansel. 2013. Fungal oxidative dissolution of the Mn(II)-bearing mineral rhodochrosite and the role of metabolites in manganese oxide formation. Environ. Microbiol. **15**: 1063–1077. doi:10.1111/1462-2920.12029

Tsukagoshi, H., W. Busch, and P. N. Benfey. 2010. Transcriptional regulation of ROS controls transition from proliferation to differentiation in the root. Cell **143**: 606–616. doi:10.1016/j.cell.2010.10.020

Van Mooy, B. A. S., and others. 2015. Major role of planktonic phosphate reduction in the marine phosphorus redox cycle. Science **348**: 783–785. doi:10.1126/science.aaa8181

Voelker, B. M., and D. L. Sedlak. 1995. Iron reduction by photoproduced superoxide in seawater. Mar. Chem. **50**: 93–102. doi:10.1016/0304-4203(95)00029-Q

Voelker, B. M., D. L. Sedlak, and O. C. Zafiriou. 2000. Chemistry of superoxide radical in seawater: Reactions with organic Cu complexes. Environ. Sci. Technol. **34**: 1036–1042. doi:10.1021/es990545x

Webb, E. A., R. W. Jakuba, J. W. Moffett, and S. T. Dyhrman. 2007. Molecular assessment of phosporus and iron physioogy in *Trichodesmium* populations from the western Central and western South Atlantic. Limnol. Oceanogr. **55**: 2221–2232. doi:10.4319/lo.2007.52.5.2221

Wuttig, K., M. I. Heller, and P. L. Croot. 2013. Pathways of superoxide (O_2^-) decay in the Eastern Tropical North

Atlantic. Environ. Sci. Technol. **47**: 10249–10256. doi: 10.1021/es401658t

Acknowledgments

We are very grateful for the assistance of the Captain and crew of the R/V *Atlantic Explorer*. We also thank Tina Thomas, Moníca Rouco, and Kyle Frischkorn for help with *Trichodesmium* collection and helpful discussion about the data. We are grateful to two anonymous reviewers, who provided thorough and constructive comments that improved this manuscript. Major support for this work was provided by NSF OCE-1246174 to CMH, NSF OCE-1332912 to STD and NSF OCE-13329898 to BASVM.

Submitted 28 August 2015
Revised 19 November 2015
Accepted 30 December 2015

Associate editor: Mary Scranton